Electronic Supplementary Material (ESI) for New Journal of Chemistry.

Electronic Supporting Information

The role of 4-halogenobenzoate ligands on luminescent and structural properties of lanthanide complexes: experimental and theoretical approaches

Jorge H.S.K. Monteiro,[†] Ana de Bettencourt-Dias,[#] Italo O. Mazali,[†] Fernando A. Sigoli,[†*]

[†] Department of Inorganic Chemistry, Institute of Chemistry, University of Campinas, Campinas, São Paulo, Brazil
[#] Department of Chemistry, University of Nevada, Reno, NV 89557

Table of contents

1. Elemental Analysis

The found and calculated % Ln^{3+}, % C and % H of the complexes are shown in Table S1.

Table S1. % Ln^{3+}, % C and % H of the complexes.

Complexes	% Ln^{3+}		% C		% H	
	found	calc.	found	calc.	found	calc.
$[Eu(4\text{-}fba)_3(H_2O)_2]$	24.5	25.1	40.52	41.67	2.32	2.66
$[Gd(4\text{-}fba)_3(H_2O)_2]\bullet 1/2H_2O$	25.4	25.4	39.68	40.71	2.44	2.77
$[Tb(4\text{-}fba)_3(H_2O)_2]\bullet 1/2H_2O$	25.7	26.3	40.87	41.81	2.83	2.51
$[Eu(4\text{-}cba)_3]\bullet 2H_2O$	22.9	23.2	39.14	38.53	2.20	2.46
$[Gd(4\text{-}cba)_3(H_2O)]$	23.3	24.5	38.90	39.29	2.56	2.20
$[Tb(4\text{-}cba)_3(H_2O)_2]$	25.9	24.0	37.52	38.12	3.00	2.44
$[Eu(4\text{-}bba)_3]\bullet 5/2H_2O$	18.8	19.1	31.33	31.65	1.69	2.15
$[Gd(4\text{-}bba)_3(H_2O)_2]$	19.7	19.8	32.40	31.80	1.58	2.03
$[Tb(4\text{-}bba)_3(H_2O)]$	20.5	20.5	32.13	32.46	1.71	1.82
$[Eu(4\text{-}iba)_3(H_2O)(dmf)]$	15.0	15.4	28.88	29.29	2.05	2.15
$[Eu(4\text{-}iba)_3(H_2O)_2]$	16.6	16.4	27.50	27.15	1.51	1.74
$[Gd(4\text{-}iba)_3(H_2O)_2]$	16.7	16.8	26.93	27.00	1.44	1.73
$[Tb(4\text{-}iba)_3(H_2O)_2]$	18.0	17.3	26.24	27.48	1.42	1.54

2. *TGA*

The TGA curves of complexes are shown in Figures S1 – S4.

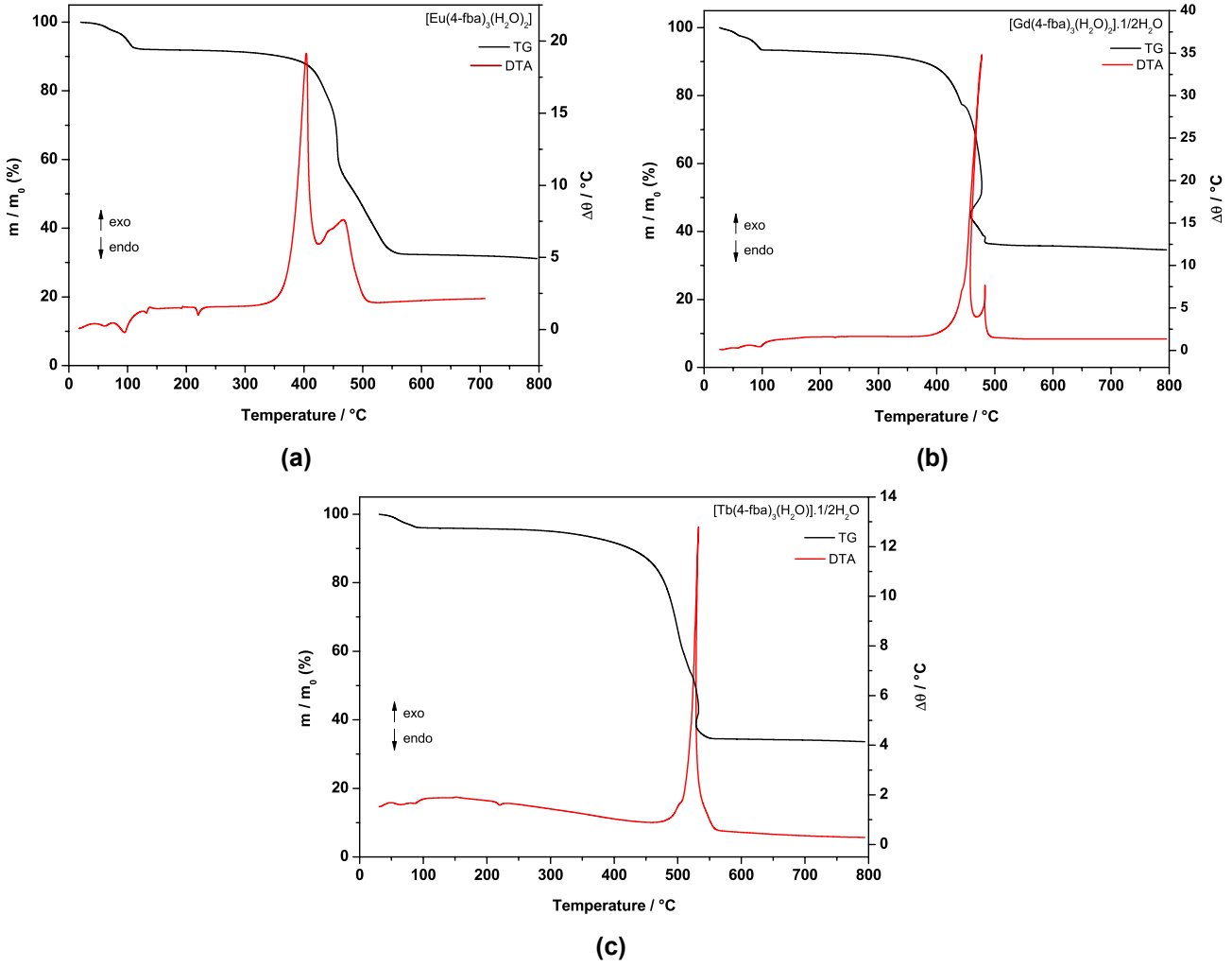

Figure S1. TGA and DTA curves of the complexes with the 4-fba ligand. (a) $[Eu(4\text{-fba})_3(H_2O)_2]$. (b) $[Gd(4\text{-fba})_3(H_2O)_2]\bullet 1/2H_2O$. (c) $[Tb(4\text{-fba})_3(H_2O)]\bullet 1/2H_2O$.

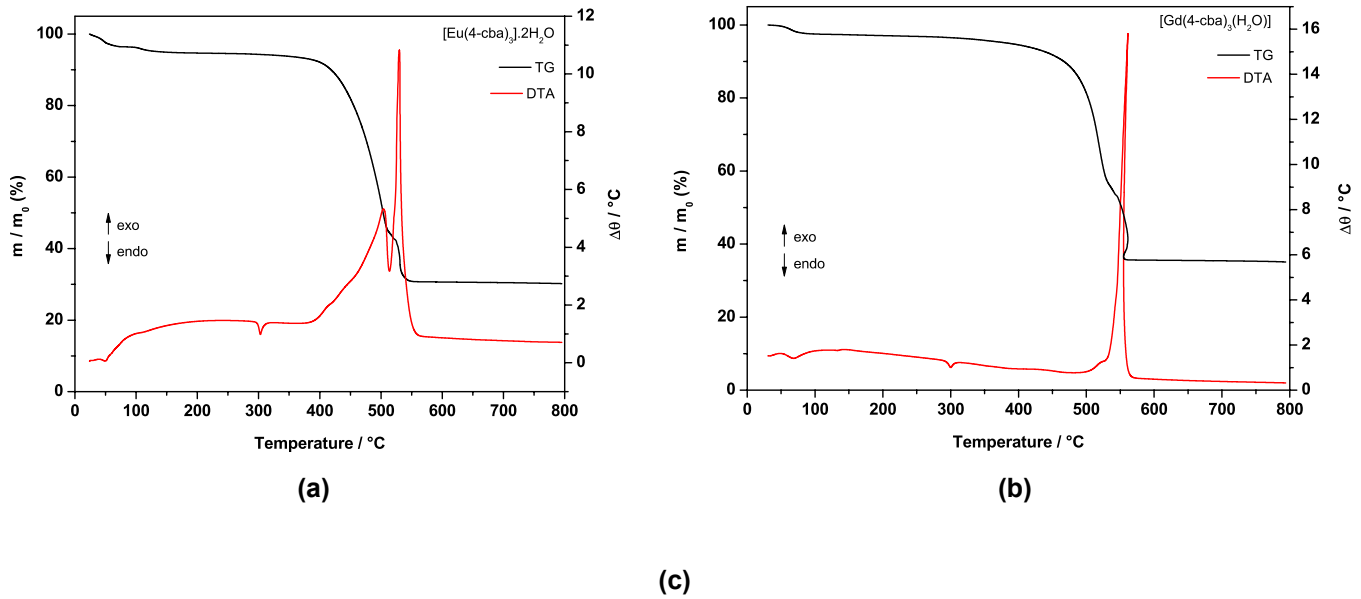

Figure S2. TGA and DTA curves of the complexes with the 4-cba ligand. (a) $[Eu(4\text{-}cba)_3]\bullet 2H_2O$. (b) $[Gd(4\text{-}cba)_3(H_2O)]$. (c) $[Tb(4\text{-}cba)_3(H_2O)_2]$.

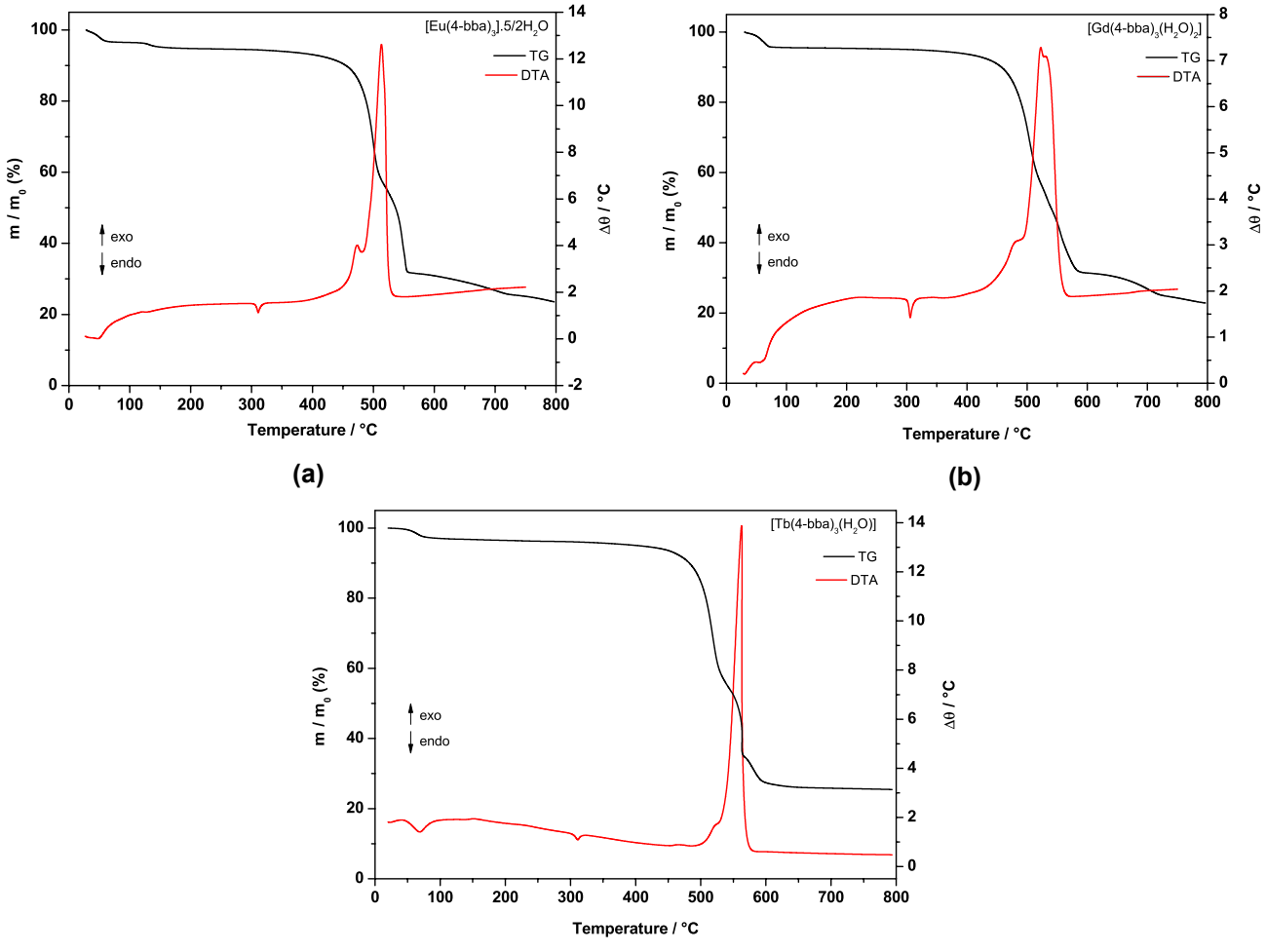

Figure S3. TGA and DTA curves of the complexes with the 4-bba ligand. (a) $[Eu(4\text{-}bba)_3]\bullet 5/2H_2O$. (b) $[Gd(4\text{-}bba)_3(H_2O)_2]$. (c) $[Tb(4\text{-}bba)_3(H_2O)]$.

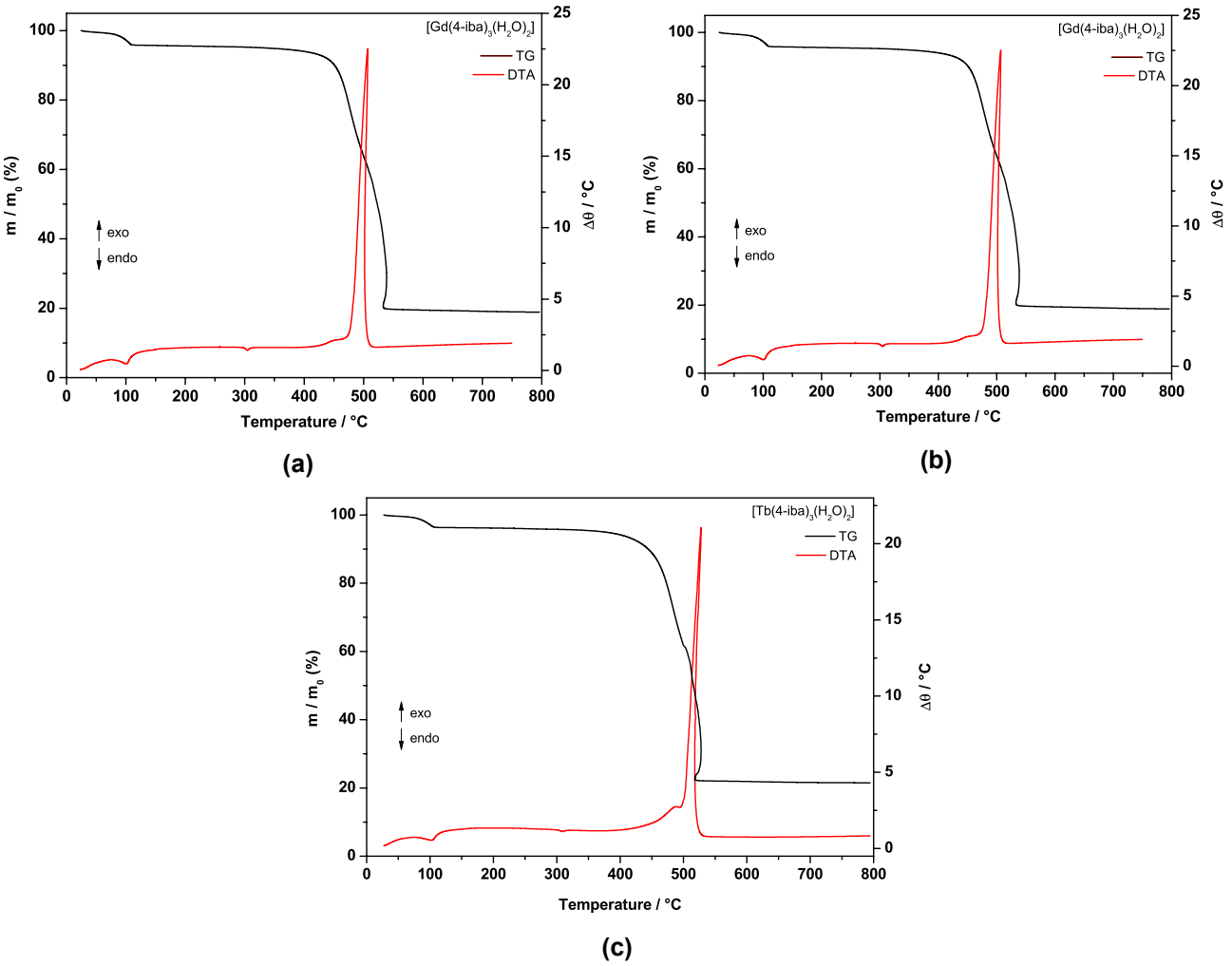

Figure S4. TGA and DTA curves of the complexes with the 4-iba ligand. (a) $[Eu(4\text{-iba})_3(H_2O)_2]$. (b) $[Gd(4\text{-iba})_3(H_2O)_2]$. (c) $[Tb(4\text{-iba})_3(H_2O)_2]$.

Table S2. Comparison between experimental and calculated weight loss for water molecules of the complexes.

Complexes	$(\Delta m)_{exp}$ / %	$(\Delta m)_{calc}$ / %
$[Eu(4\text{-fba})_3(H_2O)_2]$	4.96	5.29
$[Gd(4\text{-fba})_3(H_2O)_2]\bullet 1/2H_2O$	7.10	7.26
$[Tb(4\text{-fba})_3(H_2O)]\bullet 1/2H_2O$	4.14	4.48
$[Eu(4\text{-cba})_3]\bullet 2H_2O$	5.29	5.50
$[Gd(4\text{-cba})_3(H_2O)]$	2.48	2.81
$[Tb(4\text{-cba})_3(H_2O)_2]$	5.63	5.44
$[Eu(4\text{-bba})_3]\bullet 5/2H_2O$	5.38	5.65
$[Gd(4\text{-bba})_3(H_2O)_2]$	4.46	4.54
$[Tb(4\text{-bba})_3(H_2O)]$	2.51	2.32
$[Eu(4\text{-iba})_3(H_2O)_2]$	4.07	3.88
$[Gd(4\text{-iba})_3(H_2O)_2]$	4.17	3.85
$[Tb(4\text{-iba})_3(H_2O)_2]$	3.63	3.85

3. FT-IR

The FT-IR spectra of the complexes are shown in the Figure S6 and the $\Delta\nu$ values calculated for the sodium salt ligands and the respective complexes series are shown in Table S3. The coordination of the COO^- group was confirmed by the shift, of the $\nu_a(COO^-)$ stretching, to lower wavenumbers in the FT-IR spectra of the complexes when compared with the ligands sodium salts (Figure S6, Table S3). If the $\Delta\nu$ value for the complex is higher, similar or lower than the value of $\Delta\nu$ for the ligand salt the possible coordination modes are: monodentate, bidentate bridging or bidentate chelate, respectively[1, 2], Figure S5.

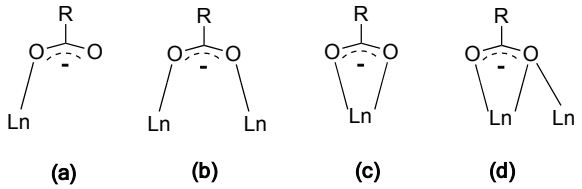

Figure S5. Coordination modes of the carboxilate ion. (a) Monodentate ($\Delta\nu_c > \Delta\nu_L$). Bidentate bridging ($\Delta\nu_c \sim \Delta\nu_L$). Bidentate chelate ($\Delta\nu_c < \Delta\nu_L$). Bidentate bridging and chelate ($\Delta\nu_{bridging} < \Delta\nu_c < \Delta\nu_{chelate}$).

For the $[Ln(4\text{-fba})_3(H_2O)_x]$ (Figure S5(a)), $[Ln(4\text{-cba})_3(H_2O)_x]$ (Figure S6(b)) complexes there is a splitting of the band attributed to the $\nu_a(COO^-)$ (~1,550 cm^{-1}) which might indicate the presence of two different coordination modes for the carboxylate group. For the $[Ln(4\text{-bba})_3(H_2O)_x]$ ((Figure S6(c)) and $[Ln(4\text{-iba})_3(H_2O)_x]$ ((Figure S6(d)) there is a shift to lower wavenumbers of the band attributed to the $\nu_a(COO^-)$ stretching and also a new band around (~1,550 cm^{-1}) which also might indicate two coordination modes for the carboxylate group. For all series of complexes ($[Ln(4\text{-fba})_3(H_2O)_x]$, $[Ln(4\text{-cba})_3(H_2O)_x]$, $[Ln(4\text{-bba})_3(H_2O)_x]$ and $[Ln(4\text{-iba})_3(H_2O)_x]$) a value for $\Delta\nu$ similar of the value obtained for the sodium salt was found (Table S3) which indicates the presence of the bidentate bridging mode. For the $[Ln(4\text{-bba})_3(H_2O)_x]$ (Figure S6(b)) and $[Ln(4\text{-iba})_3(H_2O)_x]$ (Figure S6(d)) series of complexes it was obtained a $\Delta\nu$ values smaller than the one obtained for the sodium salt (Table S3) which indicates the presence of the bidentate chelate mode. A third value for $\Delta\nu$, which is an intermediate between the value for the bidentate bridging and bidentate chelate mode, was found (Table S3) for the $[Ln(4\text{-fba})_3(H_2O)_x]$ (Figure S6(a)), $[Ln(4\text{-cba})_3(H_2O)_x]$ (Figure S6(b)) and $[Ln(4\text{-iba})_3(H_2O)_x]$ (Figure S6(d)) series of complexes. As an intermediate value this mode might be attributed to a simultaneous bidentate bridging and chelate coordination modes. Usually ligands containing the carboxylate groups show these coordination modes due to the formation of dimeric or even polymeric structures.

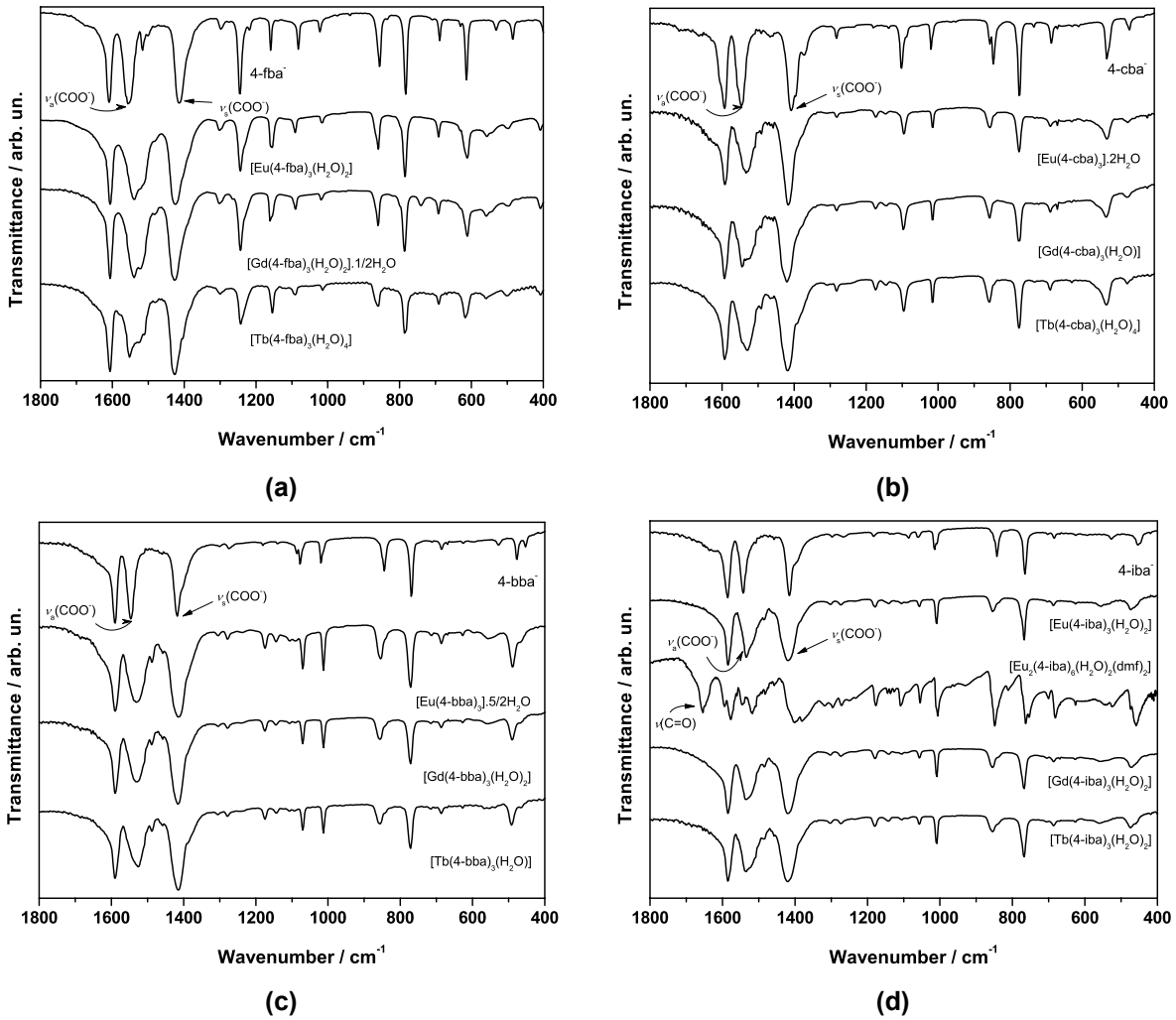

Figure S6. FT-IR spectra of the ligand sodium salts and complexes. (a) 4-fba complexes series. (b) 4-cba complexes series. (c) 4-bba complexes series. (d) 4-iba complexes series. All the complexes are indicated in the figure.

Table S3. Values of $\nu_a(COO^-)$, $\nu_s(COO^-)$ and $\Delta\nu(COO^-)$ of the ligand salts and the complexes.

Compounds	$\nu_a(COO^-)$ / cm^{-1}	$\nu_s(COO^-)$ / cm^{-1}	$\Delta\nu(COO^-)$/ cm^{-1}
Na^+4-fba$^-$	1553	1412	141
[Ln(4-fba)$_3$(H_2O)$_x$]	1541 / 1519	1427	114 / 92
Na^+4-cba$^-$	1548	1408	140
[Ln(4-cba)$_3$(H_2O)$_x$]	1543 / 1525	1419	124 / 106
Na^+4-bba$^-$	1548	1418	130
[Ln(4-bba)$_3$(H_2O)$_x$]	1530 / 1489	1414	116 / 75
Na^+4-iba$^-$	1546	1413	133
[Ln(4-iba)$_3$(H_2O)$_x$]	1531 / 1520 / 1485	1420	114 / 103 / 68

4. Gadolinium(III) complexes time resolved spectra

The energy of the triplet level (T) of the ligands were determined from the time resolved emission spectra, of analogous gadolinium(III) complexes obtained at 77 K, Figure S7. From the phosphorescence spectra, the energies of the triplet states were determined fitting a tangent at the highest energy band edge or the peak of the highest band obtained from the deconvolution of the phosphorescence spectra, Figure S8.

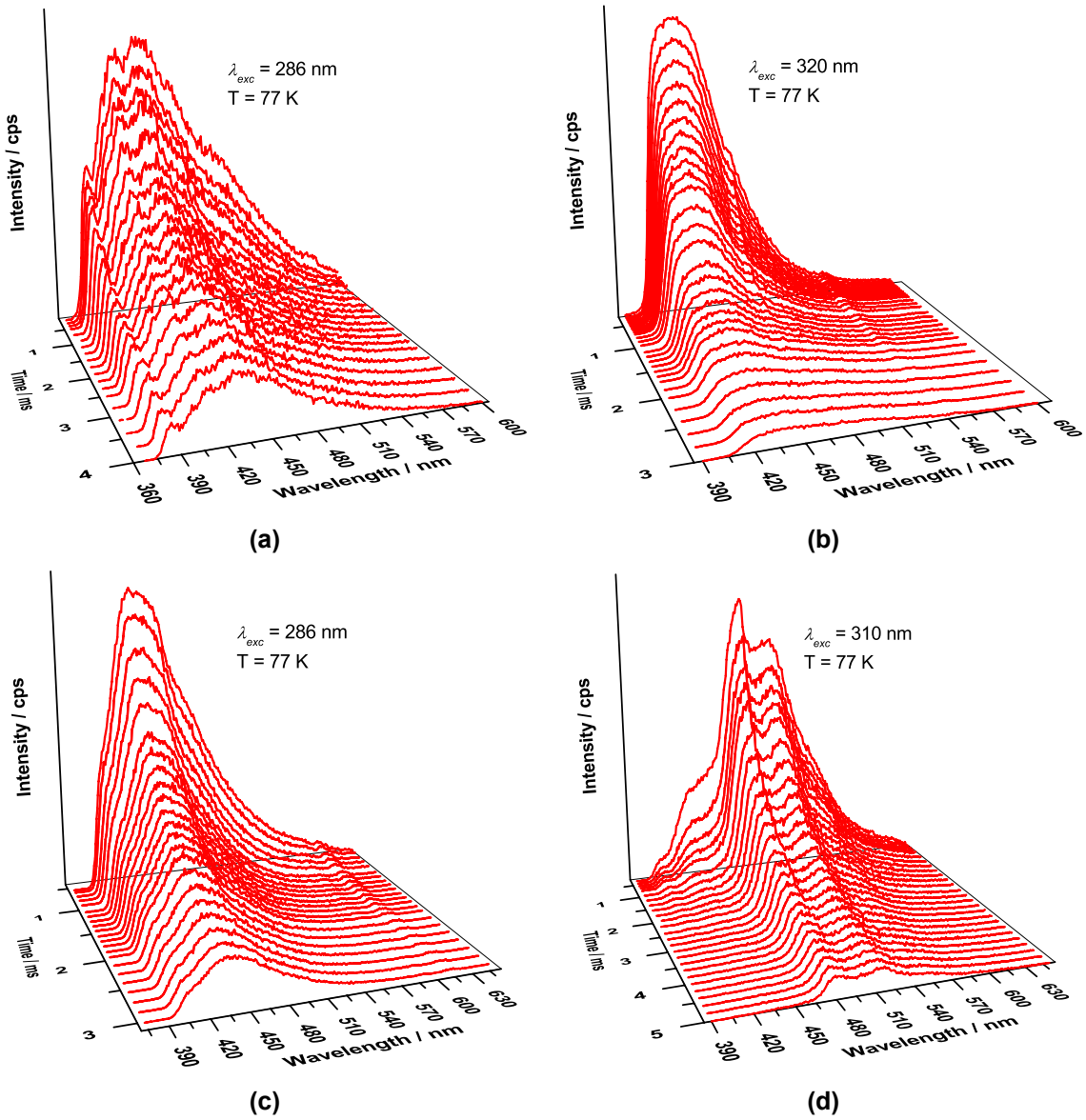

Figure S7. Time resolved emission spectra of gadolinium(III) complexes obtained at 77K. (a) $[Gd(4\text{-}fba)_3(H_2O)_2]\cdot 1/2H_2O$. (b) $[Gd(4\text{-}cba)_3(H_2O)]$. (c) $[Gd(4\text{-}bba)_3(H_2O)_2]$. (d) $[Gd(4\text{-}iba)_3(H_2O)_2]$.

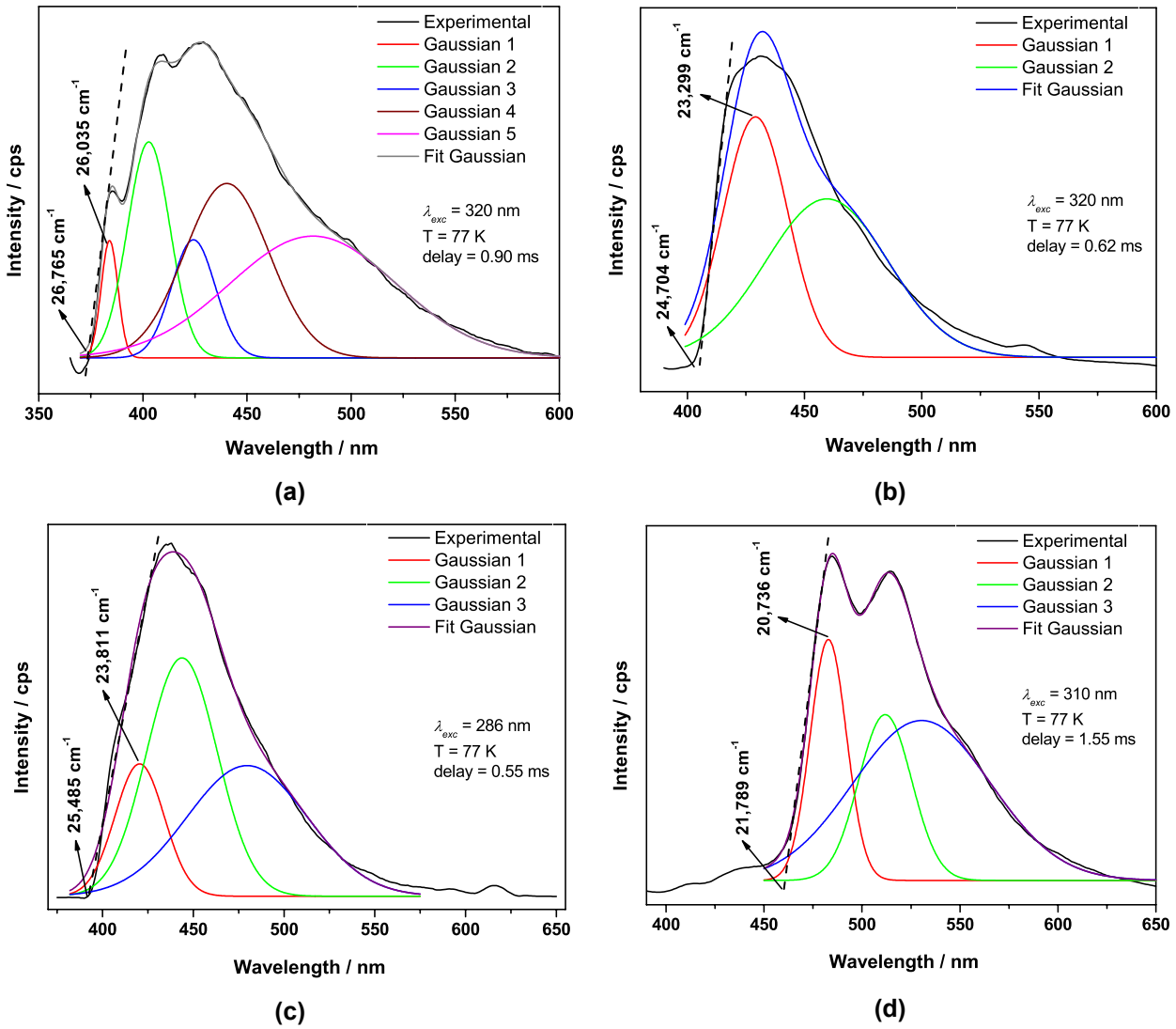

Figure S8. Deconvolution of the phosphorescence emission band of gadolinium(III) complexes obtained at 77K. (a) $[Gd(4\text{-}fba)_3(H_2O)_2]\bullet 1/2H_2O$. (b) $[Gd(4\text{-}cba)_3(H_2O)]$. (c) $[Gd(4\text{-}bba)_3(H_2O)_2]$. (d) $[Gd(4\text{-}iba)_3(H_2O)_2]$.

5. UV-Vis DRS spectra

The UV-Vis diffuse reflectance spectra of the europium(III) and gadolinium(III) complexes are shown in Figure S9. The LMCT band was obtained by the arithmetic subtraction between the europium(III) and gadolinium(III) diffuse reflectance spectra.

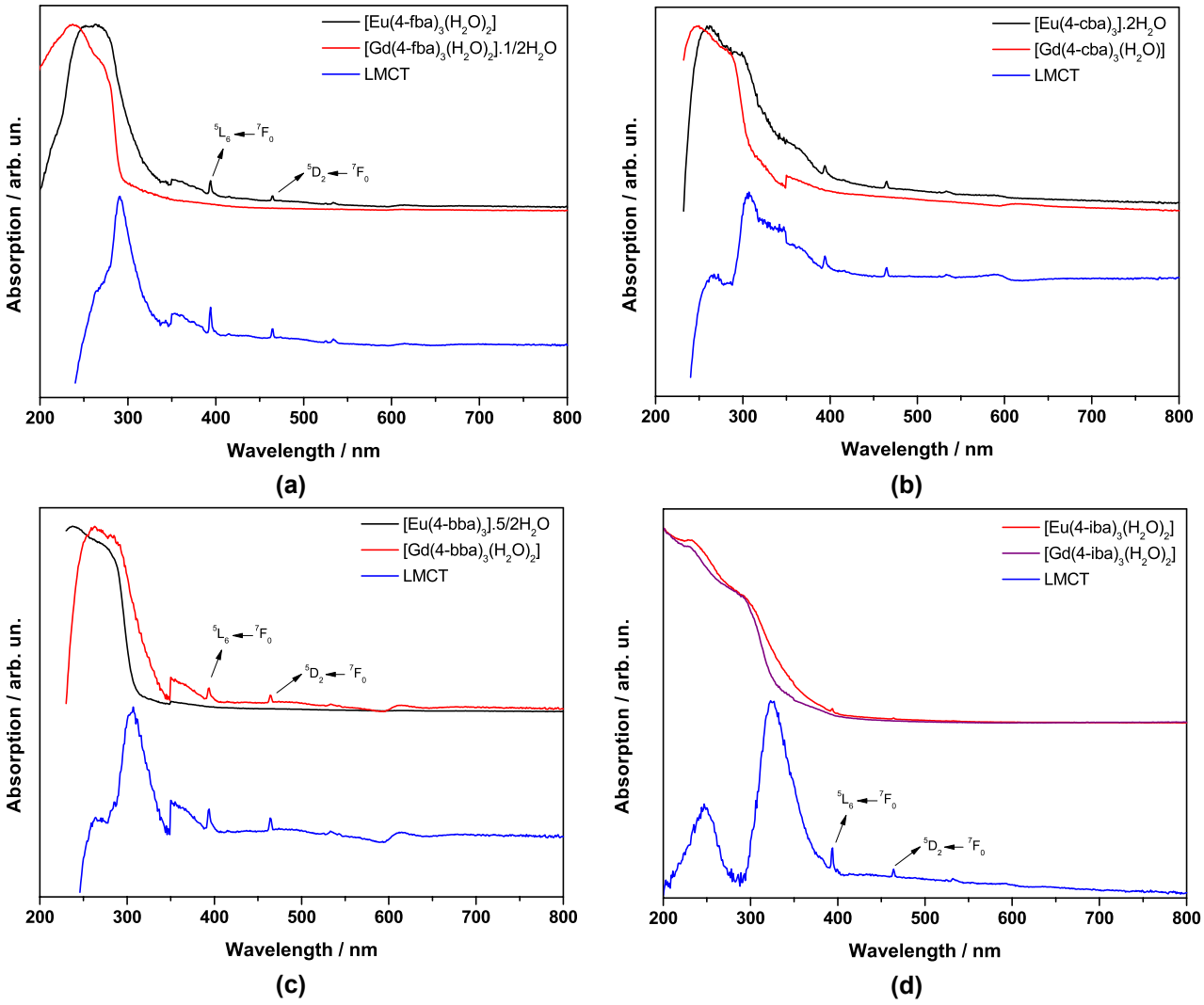

Figure S9. UV-Vis diffuse reflectance spectra of the europium(III) and gadolinium(III) complexes in the solid state. (a) 4-fba. (b) 4-cba. (d) 4-bba. (e) 4-iba

6. Decay curves

The emission decay curves and linearization for the europium(III) and terbium(III) complexes are shown in Figure S10.

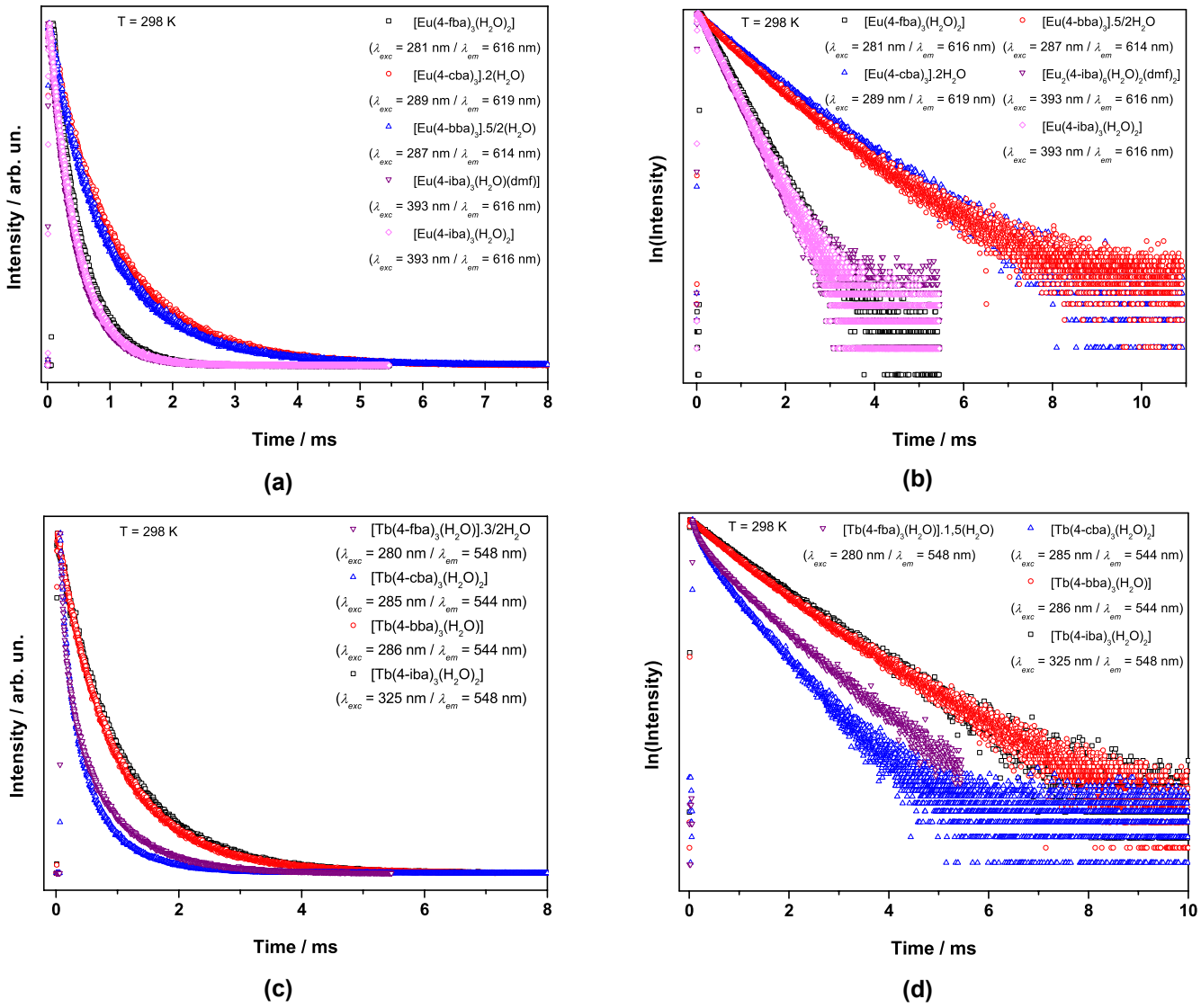

Figure S10. Emission decay curves and linearization of the curves for the complexes. (a) Emission decay curve for the europium(III) complexes. (b) Linearization of the decay curve for the europium(III) complexes. (c) Emission decay curve for the terbium(III) complexes. (d) Linearization of the decay curve for the terbium(III) complexes.

7. *Theoretical studies*

The ground states geometries of the europium(III) complexes are shown in Figure S11.

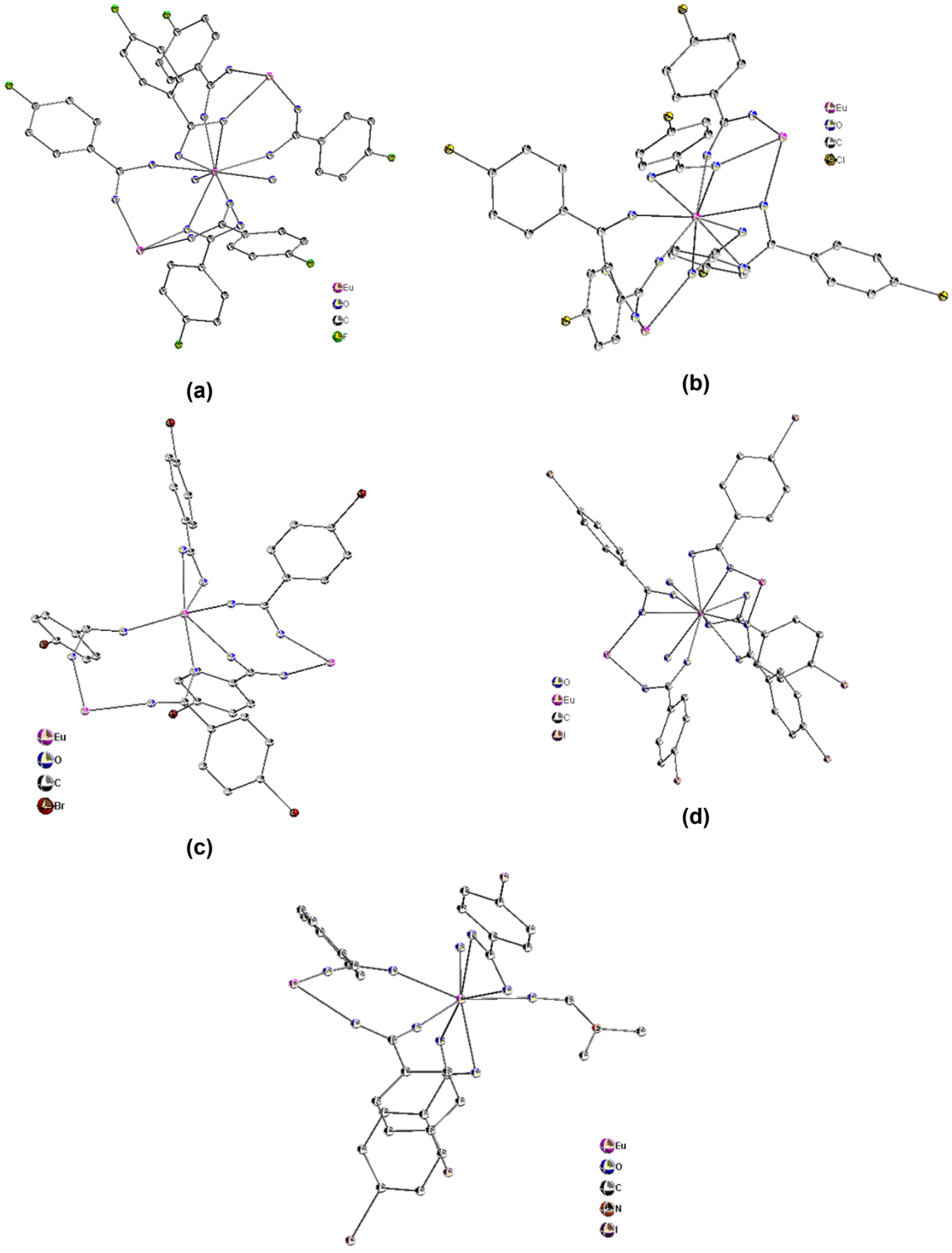

Figure S11. Ground state geometries of the europium(III) complexes. (a) $[Eu(4\text{-}fba)_3(H_2O)_2]$. (b) $[Eu(4\text{-}cba)_3]\bullet 2H_2O$. (c) $[Eu(4\text{-}bba)_3]\bullet 5/2H_2O$. (d) $[Eu(4\text{-}iba)_3(H_2O)_2]$. (e) $[Eu_2(4\text{-}iba)_6(H_2O)_2(dmf)_2]$.

Table S4. Values obtained for the *g* and α parameters. The parenthesis indicates the values for the oxygen atoms in the group 2B.

Complexes	Group 1 (bridging)		Group 2 (bridging + chelate)		Group 3 (chelate)		Group 4 (solvent)	
	g_1 / Å^3	α_1 / Å^3	g_2 / Å^3	α_2 / Å^3	g_3 / Å^3	α_3 / Å^3	g_4 / Å^3	α_4 / Å^3
$[Eu(4\text{-}fba)_3(H_2O)_2]\bullet H_2O$	0.3645	5.7891	0.1025 (1.6208)	6.3433 (5.1190)	-	-	0.6949	4.7263
$[Eu(4\text{-}cba)_3]\bullet 2H_2O$	0.0293	6.4903	0.0184 (0.0177)	6.4997 (6.4987)	-	-	-	-
$[Eu(4\text{-}bba)_3]\bullet 5/2H_2O$	1.9947	0.0052	-	-	0.0650	4.8968	-	-
$[Eu(4\text{-}iba)_3(H_2O)_2]$	0.8650	6.0541	0.1368 (1.1580)	6.3412 (5.9180)	0.8162	6.3013	0.9945	5.9062
$[Eu(4\text{-}iba)_3(H_2O)(dmf)]$ (Sparkle/PM3)	0.7300	4.7776	-	-	1.1367	6.4138	0.3826^w 0.9477^d	3.3957^w 4.1897^d
$[Eu_2(4\text{-}iba)_6(H_2O)_2(dmf)_2]$ (Single crystal)	1.0874	3.5794	-	-	0.3896	5.4440	0.3420^w 1.8102^d	4.5815^w 5.8656^d

w – water molecules. d – dmf molecules

8. References

1. G. B. Deacon and R. J. Phillips, *Coordination Chemistry Reviews*, 1980, 33, 227-250.
2. K. Nakamoto, *Infrared and Raman spectra of inorganic and coordination compounds - Part B: Applications in coordination, organometallic, and bioinorganic chemistry*, John Wiley, New York, 5th edn., 1997.